This article has been accepted for publication in a future issue of this journal, but has not been fully edited. Content may change prior to final publication. Citation information: DOI 10.1109/ACCESS.2021.3073780, IEEE Access

IEEE Access
Multidisciplinary ⋮ Rapid Review ⋮ Open Access Journal

Date of publication xxxx 00, 0000, date of current version xxxx 00, 0000.

Digital Object Identifier 10.1109/ACCESS.2017.Doi Number

Methodology for the Techno-economic Assessment of Medium-Voltage Photovoltaic Prosumers Under Net-Metering Policy

Kalliopi D. Pippi[1], Student Member, IEEE, Georgios C. Kryonidis[2], Member, IEEE, and Theofilos A. Papadopoulos[1], Senior Member, IEEE

[1]Department of Electrical and Computer Engineering, Democritus University of Thrace, Xanthi, Greece
[2]School of Electrical & Computer Engineering, Aristotle University of Thessaloniki, Thessaloniki, Greece

Corresponding author: Theofilos A. Papadopoulos (e-mail: thpapad@ee.duth.gr).

The research work was supported by the Hellenic Foundation for Research and Innovation (H.F.R.I.) under the "First Call for H.F.R.I. Research Projects to support Faculty members and Researchers and the procurement of high-cost research equipment grant" (Project Number: HFRI-FM17-229).

ABSTRACT Net-metering has been introduced as an alternative to the feed-in tariff scheme to encourage consumers to act as prosumers by installing photovoltaics. Originally, net-metering referred mainly to household photovoltaic systems, however, larger prosumers connected to medium-voltage networks are also considered. Scope of this paper is to present a techno-economic assessment methodology to evaluate the viability of net-metering policy in medium-voltage prosumers. Unlike most relevant methods, the proposed methodology combines techno-economic analysis with a quasi-static simulation model incorporating the real-world operational properties of the distribution network, where the medium-voltage prosumers are connected. The analysis focuses on nine university campuses operating under net-metering policy. The impact of several important parameters on the viability of the investment as well as on the optimal size of the system is investigated; among them special emphasis is given on the applicability of the decentralized voltage regulation techniques applied to the prosumer's photovoltaic system.

INDEX TERMS Medium-voltage, net-metering, photovoltaics, techno-economic analysis, university campuses, voltage regulation

I. INTRODUCTION

Driven by the environmental concerns on using fossil fuels for energy production, the European Union (EU) has initiated a transition towards clean and sustainable energy [1], [2]. Currently, the share of renewable energy sources (RES) in the gross final energy consumption is 19.7 % [3], revealing a large gap from the complete independence from fossil fuels. As a result, the RES share will continue to increase in the next decades by installing new units at transmission or distribution level.

Nevertheless, different factors, e.g., economic, political or technical, appear to impact the RES integration at distribution networks [4], [5]. For this reason, various support mechanisms or combinations of existing policies, e.g., tax deduction or subsidies, have been proposed to encourage end-users to act as prosumers by installing RES, and especially photovoltaics (PVs) [6] - [14]. Among them, net-metering (NEM) and net-billing (NEB) are the most widely used mechanisms, initially introduced as an alternative to the feed-in tariff (FiT) scheme [7] - [10]. Indicatively, the NEM mechanism is applied to Belgium, Cyprus, Greece [8], [11], Poland [10], etc., while the NEB is used in Italy, Mexico, etc. [12]. NEM and NEB are electricity billing mechanisms where a prosumer exploits the energy produced from a local, owned RES unit to offset the consumed energy within its premises. Assuming a given netting/billing period, the offsetting process is implemented at pre-defined timeslots, varying from few seconds up to months [7], [13]. The main difference between NEB and NEM lies on the assumed rate of the excess energy. Specifically, in NEM, the excess energy injected into the grid is charged with the same price as the consumed energy (energy compensation); in NEB it is charged at a lower price (financial compensation) [9].

However, the increasing RES penetration in distribution networks poses unprecedented technical challenges to

This work is licensed under a Creative Commons Attribution-NonCommercial-NoDerivatives 4.0 License. For more information, see https://creativecommons.org/licenses/by-nc-nd/4.0/

This article has been accepted for publication in a future issue of this journal, but has not been fully edited. Content may change prior to final publication. Citation information: DOI 10.1109/ACCESS.2021.3073780, IEEE Access

network operators, jeopardizing the reliable operation of power systems, due to e.g., power fluctuations [15], voltage rise [16], [17] and network overloading [18]. In particular, in medium-voltage (MV) networks, the voltage rise problem is one of the most important technical challenges [16], [17], [19]. Therefore, in order to limit voltage violations and ensure the reliable operation of the power system, different solutions have been proposed, including grid reinforcement [20], real power curtailment (RPC) [21], [22] and provision of reactive power by PVs [23] - [26]. However, the first solution requires significant investments, being prohibitive for distribution system operators (DSOs), while RPC results into a significant reduction of revenues, being less attractive for investors. On the other hand, voltage regulation based on reactive power control can be considered as a cost-effective solution, especially in MV networks, due to the relatively low R/X line ratio [25].

The main motivation of this paper is to present a techno-economic assessment methodology to evaluate the viability of NEM policy in MV prosumers and investigate the effect of various important parameters. The economic viability of the NEM policy regarding low-voltage (LV) residential prosumers has been well investigated in several studies [4], [7], [8], [10], [27] - [31]. However, according to the authors' knowledge there are very few relevant works regarding MV prosumers [32]. In particular, LV prosumers are charged with volumetric retail rates based on the total consumed energy (in terms of real power), assuming unity power factor (typically the case for most households) [5]. On the other hand, the electricity charging mechanism of MV prosumers is generally more complex. For example, in Greece it is based both on the total consumed energy (both in terms of real and reactive power) and real power peak demand. This also implies that the effect of reactive power voltage regulation control on electricity charge becomes important for MV prosumers, while this is not the case for LV NEM.

The proposed method is generic and can be applied to any type of MV NEM prosumers regardless the electricity charging mechanism. Nevertheless, the analysis focuses on nine campuses of the Democritus University of Thrace (DUTH) in Greece, considered as the prosumers under study. From the obtained results the viability and profitability of the NEM policy in the nine campuses is evaluated and the optimal size for the PV system is determined in terms of maximizing the net present value by applying an exhaustive search optimization procedure. The present work extends a previous study [32] that has described preliminary investigations. Additional strengths and contributions of the analysis are:

- Unlike most relevant methods, the proposed methodology combines techno-economic analysis (in terms of several indicators) with quasi-static simulations to incorporate the real-world operational properties of the distribution network; thus, improving the accuracy of the final evaluation. Annual timeseries of the real and reactive power demand as well as of the PV production from MV prosumers are used as inputs to the developed simulation model.
- Special emphasis is given on the investigation of the applicability of decentralized voltage regulation techniques contained in the PV systems and their impact on the cost-efficiency of the NEM policy.
- By using the proposed methodology, the effect of a variety of parameters is investigated to ensure adequate profitability to prosumers and facilitate the fine-tuning of policy alternatives by policy makers.

The rest of the paper is organized as follows: In Section II, the proposed methodology is presented. In Section III, the necessary information about the electricity billing mechanism and the existing NEM policy of MV costumers in Greece is described. The theoretical background of voltage regulation techniques and the techno-economic indicators used are presented in Sections IV and V, respectively. Moreover, energy demand data as well as the PV production profiles are analyzed in Section VI, while the obtained results are presented and discussed in Section VII. Finally, Section VIII summarizes the most significant conclusions of the paper.

II. METHODOLOGY

A techno-economic assessment methodology of MV prosumers under the NEM scheme is introduced following the flowchart of Fig. 1. The analysis contains the calculation of the MV prosumer's energy by taking into account the interaction with the distribution network. The viability of the NEM investment is then evaluated in terms of techno-economic indicators. In more detail the proposed methodology involves the four following steps:

1) Data initialization: the necessary data for power flow analysis and cost calculations are provided by the user as inputs to the model. Additionally, the PV size, degradation, lifetime, the voltage regulation control scheme and the electricity charging mechanism are determined.
2) Off-grid analysis: an initial estimate of the impact of the PV size on the viability of the NEM scheme is performed by means of off-grid calculations.
3) Quasi-Static analysis: quasi-static timeseries analysis is conducted on annual basis; the electricity cost of NEM charging is calculated by incorporating the effect of the network operational properties.
4) Techno-economic assessment: NEM policy is evaluated by calculating a set of technical and investment appraisal indicators. The evaluation process incorporates the NEM scheme and allows the evaluation of the optimal PV size, the effect of demand, variable PV system properties as well as the application of different voltage regulation schemes and electricity charging mechanisms; thus, the proposed methodology can be considered generic.

This work is licensed under a Creative Commons Attribution-NonCommercial-NoDerivatives 4.0 License. For more information, see https://creativecommons.org/licenses/by-nc-nd/4.0/

This article has been accepted for publication in a future issue of this journal, but has not been fully edited. Content may change prior to final publication. Citation information: DOI 10.1109/ACCESS.2021.3073780, IEEE Access

Details on the electricity charging mechanism, the examined regulation techniques and the techno-economic assessment are provided in the next sections.

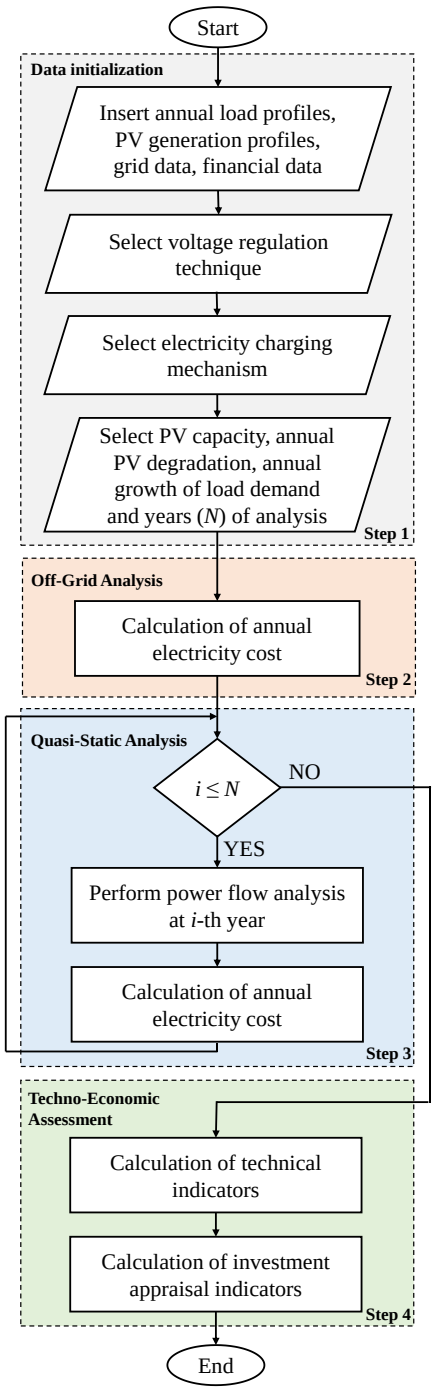

FIGURE 1. Flowchart of the proposed methodology.

III. ELECTRICITY CHARGING MECHANISM OF MV END-USERS IN GREECE

A. ELECTRICITY COST

The public power corporation (PPC) S.A. is the current major electricity supplier in Greece and offers different electricity tariffs, depending on the MV customer type. For large MV customers, e.g., commercial, industrial, campuses etc., the PPC offers specific reduced electricity pricing charged on monthly basis [32]. The total electricity tariff (C_{tot}) is subdivided into supply charges (C_{supply}), regulated charges ($C_{regulated}$) and municipal fees and taxes ($C_{municipal}$):

$$C_{tot} = C_{supply} + C_{regulated} + C_{municipal} \tag{1}$$

where:

$$C_{supply} = C_E + C_P + C_{CO_2} \tag{2}$$

$$C_{regulated} = C_{TN} + C_{DN} + C_{GhT} + C_{SGI} + C_{OC} \tag{3}$$

$$C_{municipal} = C_{MF} + C_{MT}. \tag{4}$$

In particular:

- C_{supply} is defined as the sum of the cost of energy (C_E), the cost of power (C_P) and CO_2 charges (C_{CO_2}). C_E can be calculated by analyzing the energy consumed by the customer during a billing period into two time zones, i.e., the peak and base load. The consumed energy at each time zone is evaluated at a different price. The peak time zone corresponds to the period from 7:00 to 23:00, during working days and the associated consumed energy E_A is evaluated with tariff C_{EFA}. The base load time zone corresponds to the period from 23:00 to 7:00 of working days as well as weekends and holidays. The consumed energy E_B in this zone is evaluated with price C_{EFB}.
- $C_{regulated}$ is subdivided into five categories, i.e., transmission (C_{TN}) and distribution (C_{DN}) network charges, greenhouse tax (C_{GhT}), services of general interest (C_{SGI}) and other charges (C_{OC})
- The municipal fees (C_{MF}) and taxes (C_{MT}).

A detailed analysis of the different types of economic costs is given in the Appendix.

B. NEM SCHEME

According to the NEM policy in Greece [13], the netting calculation is applied at the end of each billing period, i.e., on monthly basis for MV prosumers. Specifically, the prosumer's monthly consumed (E_{month}^{cons}) and produced (E_{month}^{prod}) energy is calculated according to (5) and (6), respectively.

$$E_{month}^{cons} = \sum_{d=1}^{D}\sum_{s=1}^{S} P_{d,s}^{cons} \cdot \Delta t \tag{5}$$

$$E_{month}^{prod} = \sum_{d=1}^{D}\sum_{s=1}^{S} P_{d,s}^{prod} \cdot \Delta t \tag{6}$$

Here, $d = 1\ldots D$ corresponds to a day of the billing period (D is the number of the days for each month), $s = 1\ldots S$ denotes the number of samples for each day d, Δt is the data

This work is licensed under a Creative Commons Attribution-NonCommercial-NoDerivatives 4.0 License. For more information, see https://creativecommons.org/licenses/by-nc-nd/4.0/

This article has been accepted for publication in a future issue of this journal, but has not been fully edited. Content may change prior to final publication. Citation information: DOI 10.1109/ACCESS.2021.3073780, IEEE Access

resolution, S is the maximum number of samples per day, i.e., S = 24 considering 1-hour (Δt) resolution data and P^{cons}, P^{prod} are the averaged consumed and produced real power of the prosumers in Δt, respectively. Since NEM does not require any synchronization between the produced and the consumed energy, the monthly netted energy of a prosumer ($E_{month}^{\text{netted}}$) is

$$E_{month}^{\text{netted}} = E_{month}^{\text{cons}} - E_{month}^{\text{prod}} + RECs_{month-1} \tag{7}$$

where *RECs* are the renewable energy credits described the excess of energy that is not directly compensated, but it is rolled over to the next period when the production is higher to the demand. *RECs* are calculated according to

$$RECs_{month} = \left[E_{month}^{\text{netted}} \right]_{-}^{(year \text{MOD} 3 \neq 0) \& (\text{month} \neq 1)} \tag{8}$$

where the operator $[\,]_{-}$ defines the projection on the negative orthant. The timeframe of rolling *RECs* is limited to the corresponding netting period, i.e., 3 years. Any excess of energy after the 3-year period is not compensated and not credited to the next account [13]; the maximum duration of the NEM contract is 25 years. In case the prosumer's production is lower than demand, the prosumer is charged on the consumed net energy ($E_{month}^{\text{charged}}$) as

$$E_{month}^{\text{charged}} = \left[E_{month}^{\text{netted}} \right]_{+} \tag{9}$$

where the operator $[\,]_{+}$ defines the projection on the positive orthant. Note that, the C_{SGI} calculation is based on the total consumed energy (E_{month}^{cons}); the rest of the regulated charges are calculated on the basis of the imported energy from the grid. The same procedure also applies to LV prosumers with differences only on the billing and netting period.

IV. VOLTAGE REGULATION TECHNIQUES

One of the most important technical challenges in modern distribution networks, due to the increasing PV penetration, is voltage rise. This is more evident, when no control scheme is used by PV systems. To mitigate the related voltage violations and ensure the reliable operation of the power system, various decentralized control schemes have been proposed in literature [23] - [26]; among them, the provision of reactive power by PVs is one of the most common approaches. In this paper, three types of decentralized control schemes are examined:

- $Q(P)$ control scheme [23]: reactive power is a linear function of the injected real power. This linear relationship between Q and P forces the PVs to operate with constant power factor. The corresponding characteristic curve is depicted in Fig. 2. PV systems with a lagging power factor absorb reactive power to mitigate the voltage rise due to increased real power injection. On the other hand, a leading power factor is applied to provide reactive power to the network and support the voltage profile under heavily loading conditions.
- $\cos\varphi(P)$ control scheme [23]: this droop-based method is more generic and provides dynamic voltage regulation compared to the $Q(P)$ control scheme since the power factor varies with respect to the injected real power improving reactive power compensation [23], [24]. It has been already adopted by some European Union grid codes [25]. The $\cos\varphi(P)$ characteristic is presented in Fig. 2. Note that, p_1, p_2, and p_3 are the real power thresholds, $\cos\varphi_{min}$ is the minimum power factor and p_{inj} is the injected real power of the PV referred to nominal conditions.
- $Q(V)$ control scheme [26]: it is one of the most common dynamic decentralized voltage regulation methods, already incorporated in the Italian, North American and English grid codes [25]. The $Q(V)$ droop characteristic is depicted in Fig. 3. In this control scheme, the reactive power of the PV systems is adjusted according to the voltage at the point of interconnection (POI) with the grid [25], [26]. Here, **QV**={V_1, V_2, V_3, V_4} is the set of the voltage thresholds, V_{POI} is the voltage at POI and $Q_{\max}$ is the maximum permissible reactive power of the PV unit [34].

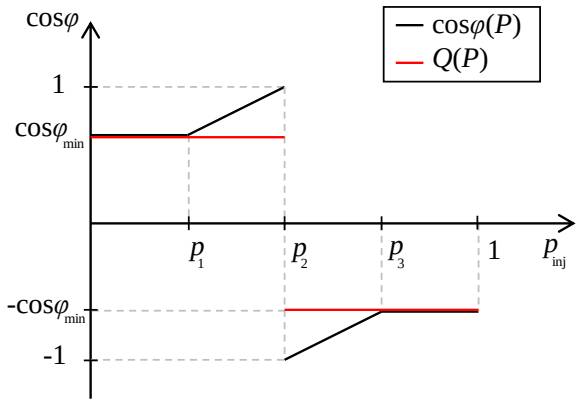

FIGURE 2. ***Q(P)* and *cosφ(P)* control schemes. Negative sign indicates lagging power factor.**

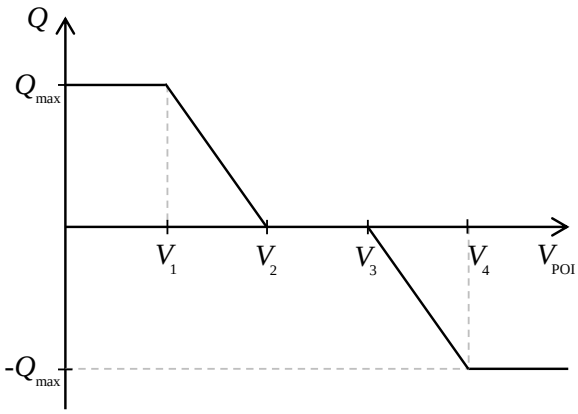

FIGURE 3. **Droop characteristic of the *Q(V)* control scheme. Negative sign indicates lagging power factor.**

This work is licensed under a Creative Commons Attribution-NonCommercial-NoDerivatives 4.0 License. For more information, see https://creativecommons.org/licenses/by-nc-nd/4.0/

This article has been accepted for publication in a future issue of this journal, but has not been fully edited. Content may change prior to final publication. Citation information: DOI 10.1109/ACCESS.2021.3073780, IEEE Access

V. TECHNO-ECONOMIC ASSESSMENT

The technical and economic assessment of the feasibility and viability of NEM policy in MV prosumers operating under different voltage regulation schemes is based on the calculation of a set of indicators described in the next sub-sections.

A. TECHNICAL INDICATORS

In literature, two main indicators have been proposed to evaluate the sizing of the PV system according to the prosumer's load profile. The self-consumption rate (*SCR*), evaluating the PV produced energy directly consumed on-site, given by [35]

$$SCR = \frac{C}{B+C} \tag{10}$$

and the self-sufficiency rate (*SSR*), related to the load energy covered by the PV production, defined as follows [35]

$$SSR = \frac{C}{A+C} \tag{11}$$

where *A*, *B*, and *C* denote the load energy covered by the grid (import energy), the excess of the PV produced energy (export energy) and the self-consumed energy, respectively.

B. INVESTMENT APPRAISAL INDICATORS

The economic viability of the NEM policy is evaluated by calculating the net present value (*NPV*), the internal rate of return (*IRR*), the discounted payback period (*DPP*), the return on investment (*ROI*) and the levelized cost of electricity (*LCOE*) indicators.

NPV stands for the difference between the present value of cash inflows and outflows over the system lifetime (*N*) and is calculated as follows [7]:

$$NPV = -I_o + \sum_{n=1}^{N} \frac{(C_n - OM_n)(1+f)^{n-1}}{(1+d)^n} \tag{12}$$

where I_o denotes the capital investment cost; OM_n and C_n stand for the operation - maintenance and savings at year *n*, respectively; *d* is the discount rate and *f* denotes the inflation rate. In this work, the net value is the savings in energy billing due to the NEM policy.

IRR estimates the profitability of the investment [7]. In particular, *IRR* is calculated in (13) by setting *NPV* equal to zero and solve (12) for the unknown *IRR* value of *d* as

$$NPV\big|_{d=IRR} = 0 \Rightarrow -I_o + \sum_{n=1}^{N} \frac{(C_n - OM_n)(1+f)^{n-1}}{(1+IRR)^n} = 0 \tag{13}$$

DPP is the required time period for the repayment of the original investment as results from (14) [7].

$$NPV\big|_{N=DPP} = 0 \Rightarrow -I_o + \sum_{n=1}^{DPP} \frac{(C_n - OM_n)(1+f)^{n-1}}{(1+d)^n} = 0 \tag{14}$$

ROI calculates the return of the investment compared to the initial cost and is given by [28]

$$ROI = \frac{NPV}{I_o}. \tag{15}$$

Finally, *LCOE* is considered as the minimum constant price at which electricity must be sold in order to compensate the investment, and is calculated by (16) [8]

$$LCOE = \left(I_o + \sum_{n=1}^{N} \frac{OM_n}{(1+d)^n} \right) \Big/ \sum_{n=1}^{N} \frac{E_n}{(1+d)^n} \tag{16}$$

where E_n is the energy yield of the PV system at year *n*.

VI. DISTRIBUTION SYSTEM SIMULATION MODEL

A. SYSTEM UNDER STUDY

Annual quasi-static timeseries simulations of 1-h resolution (8760 samples) are conducted using the Open Distribution System Simulator (OpenDSS) software [36]. A modified version of the 33-bus benchmark distribution network [37] is used as shown in Fig. 4; the number in the brackets denotes the network node number. The voltage at the slack bus is considered equal to 1.05 pu. Two main groups of end-users are considered at the 32 network nodes. The first group consists of residential and commercial loads (denoted with black and grey colour respectively); details on the used normalized timeseries are provided in Section VI.B.1. The second group corresponds to the MV prosumers, i.e., the nine university campuses (denoted with blue colour). Given the load profile characteristics and rated real power (see Section VI.B.2.) of the MV prosumers, the rated real and reactive power of the residential and the commercial loads have been adjusted (see Table I) so that the load real and reactive power at node 1 of the modified network being equal to that of the original benchmark system. Additionally, nodes 5, 9 and 15 (denoted with green) contain PV power stations. PV systems operating under NEM apply to prosumers (denoted with blue), assuming varying rated power. The load and generation profiles at each node are obtained by multiplying the rated power of each load or PV unit with the corresponding normalized profile.

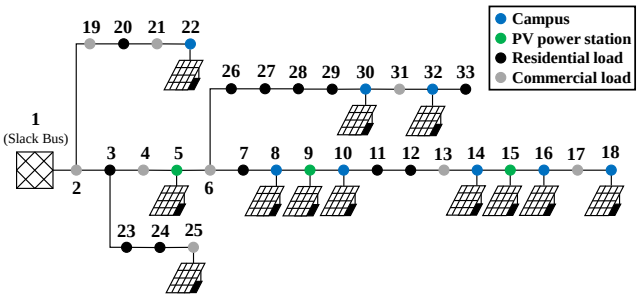

FIGURE 4. Single-line diagram of the examined network.

This work is licensed under a Creative Commons Attribution-NonCommercial-NoDerivatives 4.0 License. For more information, see https://creativecommons.org/licenses/by-nc-nd/4.0/

This article has been accepted for publication in a future issue of this journal, but has not been fully edited. Content may change prior to final publication. Citation information: DOI 10.1109/ACCESS.2021.3073780, IEEE Access

TABLE I
LOAD REAL AND REACTIVE POWER OF THE MODIFIED NETWORK

Node No.	Real Power (kW)	Reactive Power (kVAr)
2	43.23	48.49
3	38.91	32.33
4	51.88	64.66
5	25.94	24.25
6	25.94	16.16
7	86.47	80.82
9	25.94	16.16
11	19.46	24.25
12	25.94	28.29
13	25.94	28.29
15	25.94	8.08
17	25.94	16.16
19	38.91	32.33
20	38.91	32.33
21	38.91	32.33
23	38.91	40.41
24	181.59	161.65
26	25.94	20.21
27	25.94	20.21
28	25.94	16.16
29	51.88	56.58
31	64.86	56.58
33	25.94	32.33

B. LOAD TIMESERIES

1) RESIDENTIAL AND COMMERCIAL DEMAND DATA

Annual electricity profiles from the National Renewable Energy Laboratory (NREL) dataset are used. Specifically, electricity data of the West Coast region of USA are selected, since this region presents high resemblance to the Mediterranean climate [38]. In particular, fourteen residential and nine commercial load profiles are randomly applied to the network nodes. The corresponding normalized daily average profiles (24 samples) are summarized in Fig. 5.

2) UNIVERSITY CAMPUSES DEMAND DATA

The examined university campuses of DUTH are located in four cities of Thrace, i.e., Xanthi, Komotini, Alexandroupoli and Orestiada. Details regarding the capacity contract of each university campus, as well as the node of each campus connected to the modified 33-bus system are given in Table II. Aggregated daily electricity demand data for both the real and the reactive power of the nine DUTH campuses are recorded from January 2014 to December 2014 by using the online metering system of the Greek DSO [39]. In Fig. 6, the average daily demand profile of each campus is presented. It can be seen that campuses Komotini, Makri, Kimmeria and Q. Sophia present the highest demand; the rest five campuses present significantly lower demand level.

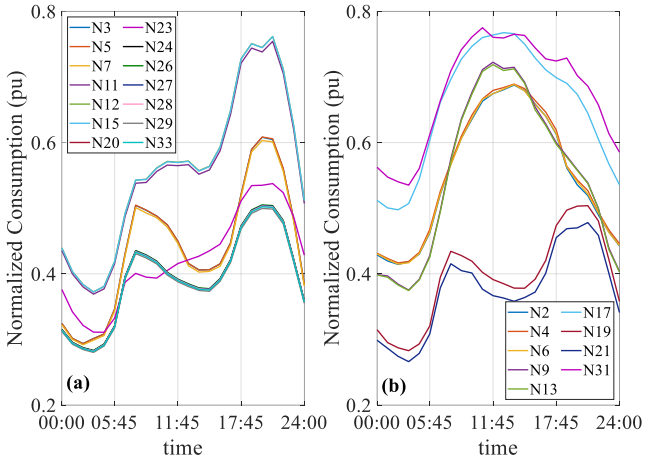

FIGURE 5. Average daily demand profile of (a) residential load profiles, (b) commercial load profiles.

TABLE II
UNIVERSITY CAMPUS DATA

Name of campus (City)	Capacity contract (kW)	Peak Load Demand (kW)	Node No.
Komotini (Komotini)	1500	987	25
Tsaldari (Komotini)	500	165	14
Makri (Alexandroupoli)	1500	480	32
Chili (Alexandroupoli)	400	137	18
Q. Sophia Str. (Xanthi)	1300	310	8
Dep. of Civil Eng. (Xanthi)	1600	102	10
Kimmeria (Xanthi)	800	350	30
Evripidou (Orestiada)	1250	83	16
Orestias (Orestiada)	650	118	22

C. PV TIMESERIES

Regarding PV generation, the online calculation tool of [40] is used, allowing to perform simulations of the hourly power output from PV installations located anywhere in the world. Five different annual PV generation timeseries have been generated; one for each city (four in total) and one common for the PV power station generation (random location in Thrace region). In Fig. 7 the average daily power (scaled to 1 kW, i.e., 1 per unit (pu)) for each city of DUTH and the PV power stations are illustrated, assuming

This work is licensed under a Creative Commons Attribution-NonCommercial-NoDerivatives 4.0 License. For more information, see https://creativecommons.org/licenses/by-nc-nd/4.0/

This article has been accepted for publication in a future issue of this journal, but has not been fully edited. Content may change prior to final publication. Citation information: DOI 10.1109/ACCESS.2021.3073780, IEEE Access

35° tilt, 180° azimuth and 10 % total PV system losses. In general, all PV generation profiles are practically similar, since the examined PV systems are located at the same geographical region.

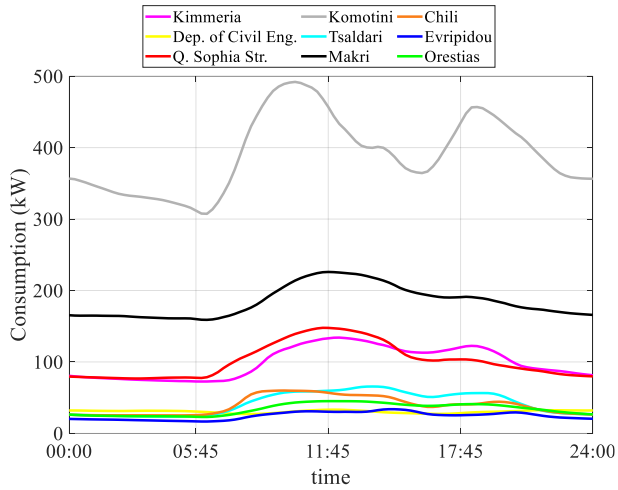

FIGURE 6. Average daily demand profiles of DUTH campuses.

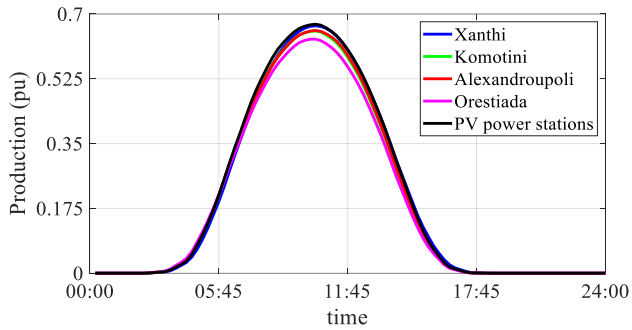

FIGURE 7. Average daily production profiles.

VII. RESULTS

The proposed techno-economic assessment methodology is employed to evaluate the profitability of NEM policy in prospective MV prosumers. An investigation on PV optimal sizing, as well as on the effect of the PV cost and voltage regulation properties on the viability of the PV system is presented.

A. TECHNO-ECONOMIC PARAMETERS

A 21-year techno-economic analysis is performed, assuming d = 5 % and f = 2 %. Prosumers are charged with the electricity tariff described in Section III; the corresponding cost category prices, including VAT (6 %), are summarized in Table III. An additional fee of 992 € for the connection of the PV system to the grid is also taken into consideration [13]. PV system costs (including 24 % VAT) are presented in Table IV. In particular, the PV module cost (€/kWp) is given as a function of PV size, PV_{size}, according to the empirical formulae of (17).

$$PV_{cost} = 818.4 - 0.248 \cdot PV_{size}. \quad (17)$$

Note that, (17) has been derived by applying linear interpolation to known PV_{size} – cost data sets, ranging from 300 kWp – 0.6 €/W to 550 kWp – 0.5 €/W, respectively; the average PV module cost is 550 €/kW. Additionally, the annual growth of the load demand and the annual PV degradation are considered, assuming 1 % and 2 % rate, respectively. Finally, the properties of the examined voltage regulation strategies are summarized in Table V.

TABLE III
TARIFF CHARGES OF THE ELECTRICITY TARIFF SCHEME

Type of Cost	€ / kWh
C_{EF_A}	0.074677
C_{EF_B}	0.0588088
UC_{vc}	0.003074
UC_{OC}	0.0000742
UC_{GhT}	0.0093068
UC_{SGI}	0.018974
Type of Cost	**€ / kW / month**
C_{PF}	7.0596
UC	1.40874
UC_{fc}	1.24974

TABLE IV
PV SYSTEM COST ANALYSIS

Type of Cost	€ / kWp
PV Module	Eq. (17)
Inverter	350
Balance of System	65
Installation & Administrative	115
O&M	3 % (of the overall cost)

TABLE V
VOLTAGE REGULATION PROPERTIES

$Q(V)$		$\cos\varphi(P)$		$Q(P)$	
V_1 (pu)	0.95	$\pm\cos\varphi_{min}$	±0.85	$\pm\cos\varphi_{min}$	±0.85
V_2 (pu)	0.96	p_1 (pu)	0.12		
V_3 (pu)	1.04	p_2 (pu)	0.5		
V_4 (pu)	1.05	p_3 (pu)	0.88		

B. OFF-GRID ANALYSIS

An initial estimate of the impact of PV_{size} on the viability of the NEM scheme for the nine DUTH campuses is performed by means of off-grid simulations. First, the technical indicators are computed by varying PV_{size} from 50 to 1000 kW. Note that, according to the Greek

This work is licensed under a Creative Commons Attribution-NonCommercial-NoDerivatives 4.0 License. For more information, see https://creativecommons.org/licenses/by-nc-nd/4.0/

This article has been accepted for publication in a future issue of this journal, but has not been fully edited. Content may change prior to final publication. Citation information: DOI 10.1109/ACCESS.2021.3073780, IEEE Access

legislation [11], [13], PV_{size} for MV prosumers can reach up to 100 % of the installation capacity contract; however, it cannot exceed 1000 kWp. In the off-grid analysis, the imported and exported energy to the grid are calculated by employing only the corresponding campus demand and PV timeseries. Figs. 8(a) and 8(b) demonstrate the *SCR* variation against PV_{size} for the 1st and 21st year of the investment, respectively. It can be generally deduced that, for all campuses *SCR* is a decreasing function of PV_{size}. For campuses presenting high demand, e.g., Komotini and Makri, high *SCR* is generally observed. On the contrary, for campuses with low demand, i.e., Tsaldari, Chili, Dep. of Civil Eng., Evripidou and Orestias, high *SCR* values are obtained only for PV_{size} lower than 200 kW. By comparing the *SCR* results of Figs. 8(a) and 8(b), it can be realized that the *SCR* for the 21st year of the investment is higher compared to the corresponding of the 1st year. This is attributed to the higher rate of PV module degradation than the annual load demand growth. Accordingly, in Fig. 9(a) and 9(b) the *SSR* variation against PV_{size} is presented for the 1st and 21st year of the analysis, respectively. It should be indicated that the findings of the *SCR* apply also for *SSR*.

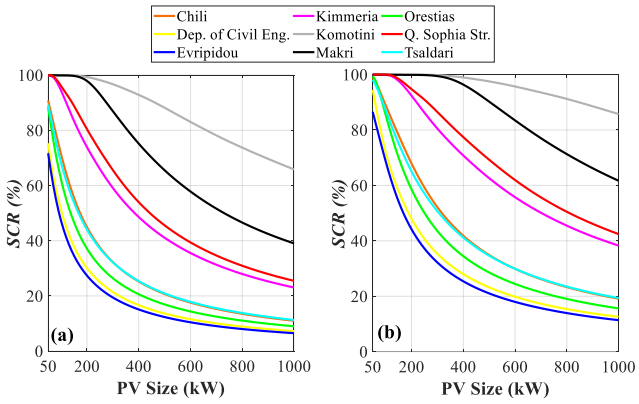

FIGURE 8. ***SCR* as a function of PV_{size}. Results for the (a) 1st and (b) 21st year of the analysis.**

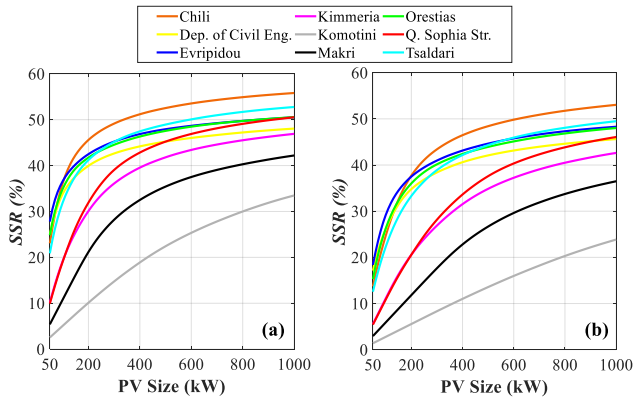

FIGURE 9. ***SSR* as a function of PV_{size}. Results for the (a) 1st and (b) 21st year of the analysis.**

The *SCR and SSR* analyses reveal that under certain conditions NEM may become attractive. Therefore, at the next step the viability of the PV system is examined by means of the investment appraisal indicators. In Fig. 10, the variation of the *NPV* against PV_{size} is analyzed. Results are grouped to campuses presenting low (Fig. 10(a)) and high (Fig. 10(b)) demand, respectively. Note that, the PV_{size} is assumed ranging from 50 kW to values yielding positive *NPV*. It can be generally seen that *NPV* increases with the PV_{size} up to a certain extent; for higher values, *NPV* starts decreasing. This is attributed to the additional PV system cost that cannot be depreciated, since the excess of the produced energy is not compensated at the end of the netting period.

Fig. 11 illustrates *IRR* as a function of PV_{size}. In the same figure the discount rate limit is also provided. Results show that *IRR* is generally a decreasing function of PV_{size}. For *IRR* higher than *d*, *NPV* is positive, thus the investment is viable. On the contrary, for *IRR* lower than *d*, *NPV* becomes negative and the investment is not considered profitable.

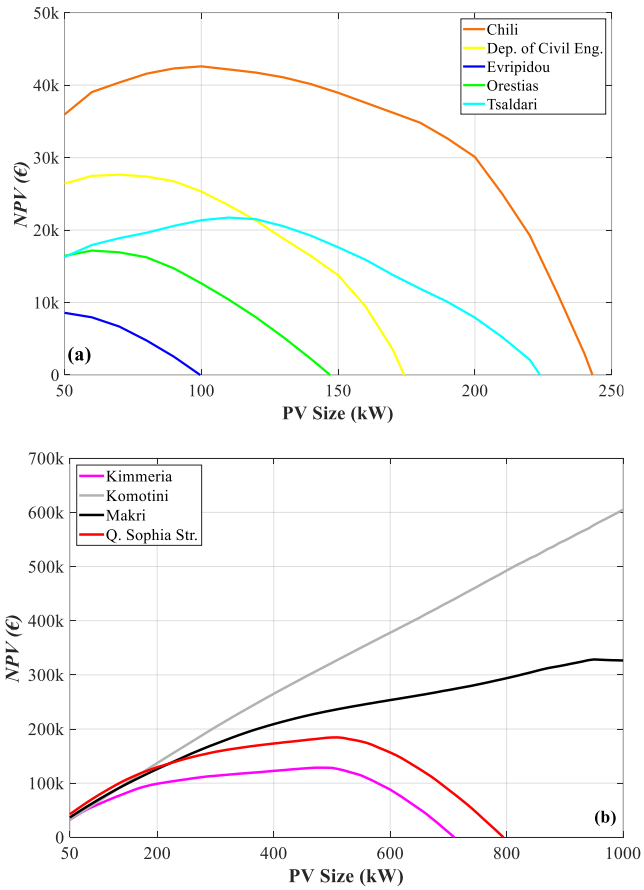

FIGURE 10. ***NPV* as a function of PV_{size} for campuses with (a) low and (b) high demand levels.**

This work is licensed under a Creative Commons Attribution-NonCommercial-NoDerivatives 4.0 License. For more information, see https://creativecommons.org/licenses/by-nc-nd/4.0/

This article has been accepted for publication in a future issue of this journal, but has not been fully edited. Content may change prior to final publication. Citation information: DOI 10.1109/ACCESS.2021.3073780, IEEE Access

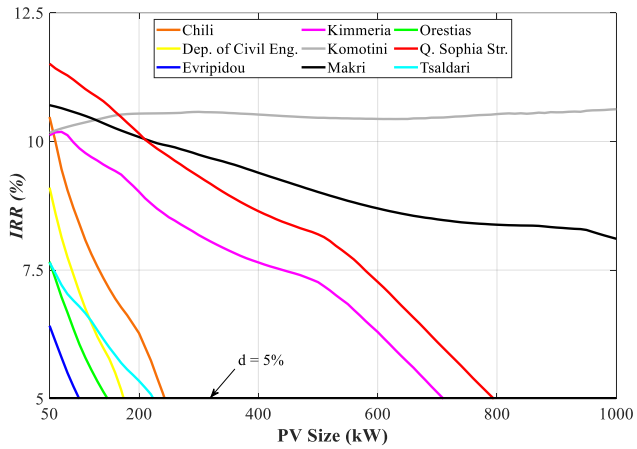

FIGURE 11. ***IRR*** **as a function of** PV_{size}**.**

The variation of *DPP* is presented in Fig. 12. Generally, *DPP* increases with PV_{size}. It should be also indicated that, for all examined cases *DPP* acquires values higher than 10 years. Additionally, the variation of the corresponding *ROI* against PV_{size} is illustrated in Fig. 13. It is evident that *ROI* is a decreasing function of PV_{size}. For cases that the investment is considered viable, *ROI* becomes positive and vice versa.

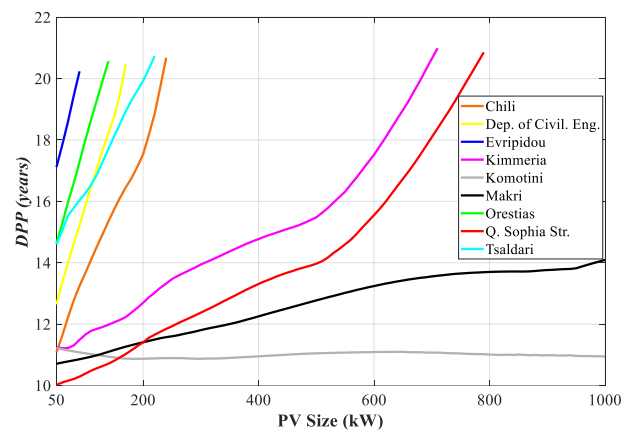

FIGURE 12. ***DPP*** **as a function of** PV_{size}**.**

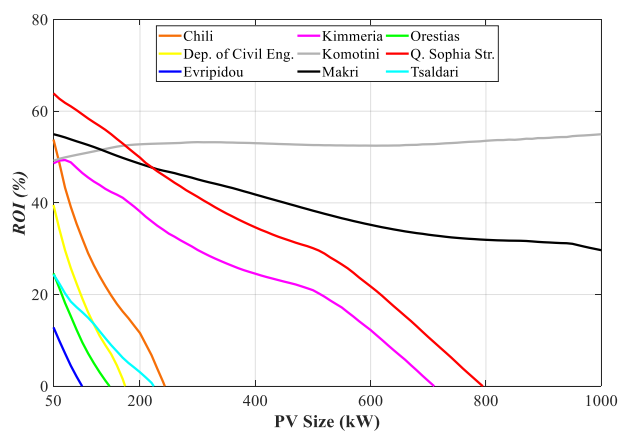

FIGURE 13. ***ROI*** **as a function of** PV_{size}**.**

Finally, in Fig. 14 *LCOE* is calculated for the cities of Xanthi, Komotini, Alexandroupoli and Orestiada. It is shown that *LCOE* decreases almost linearly with PV_{size}, due to the higher annual produced energy. This linear behavior is associated with the PV cost variation against PV_{size}, as determined by (17). Comparative analysis for the four cities shows that Xanthi yields the lowest *LCOE*; this is evident, since according to Fig. 7 this case corresponds to the highest PV production. Moreover, it can be realized that grid parity in Xanthi is achieved for all PV_{size} cases by comparing the values of Table III with *LCOE*. However, in Alexandroupoli Komotini and Orestiada the grid parity is achieved when PV_{size} is higher than 65 kWp, 80 kWp and 270 kWp, respectively.

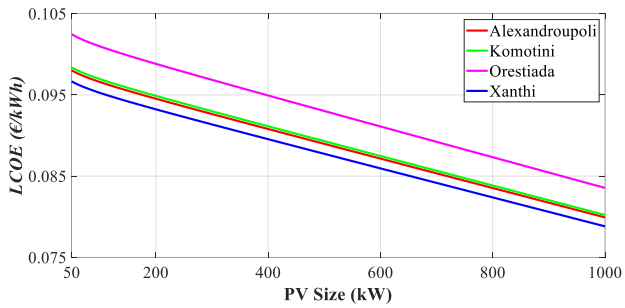

FIGURE 14. ***LCOE*** **as a function of** PV_{size}**.**

1) OPTIMAL PV SIZING

Based on the results of Fig. 10, it can be deduced that the adopted *NPV* analysis against PV_{size} can be used as an exhaustive search optimization procedure to determine the optimal PV_{size} in terms of maximizing the prosumer's profitability [31], [32].

In this context, the resulting *NPV* and *DPP* calculations are summarized in Table VI for all examined campuses. Results are also compared to those obtained by applying a simplifying approach. In this approach, the PV_{size} is determined by equalizing the PV energy production (E_{PV}) with the corresponding demand (E_{demand}). This assumption is based on the fact that any excess of energy is not compensated at the end of the netting period [13]. It is shown that for campuses presenting high demand *NPV* is indeed maximized when the generated energy tends to become equal to prosumer's demand [13]. The average repayment period for these campuses is ~15 years, i.e., within the expected range regarding investments related with primary distribution grids. However, this is not evident for campuses presenting low demand, since prosumer's profit for the examined investment lifetime period cannot result into a full (Evripidou and Orestias) or significant (Tsaldari, Chili and Dep. of Civil Eng.) repayment of the capital investment.

This work is licensed under a Creative Commons Attribution-NonCommercial-NoDerivatives 4.0 License. For more information, see https://creativecommons.org/licenses/by-nc-nd/4.0/

This article has been accepted for publication in a future issue of this journal, but has not been fully edited. Content may change prior to final publication. Citation information: DOI 10.1109/ACCESS.2021.3073780, IEEE Access

TABLE VI
NPV AND *DPP* FOR DUTH CAMPUSES

Campus	Maximum *NPV*			$E_{PV} = E_{demand}$		
	PV_{size} (kW)	*NPV* (€)	*DPP* (years)	PV_{size} (kW)	*NPV* (€)	*DPP* (years)
Komotini	1000	604,900	10.94	1000	604,900	10.94
Tsaldari	110	21,722	16.53	213	4,024	20.47
Makri	950	328,430	13.82	925	323,549	13.79
Chili	100	42,595	13.66	197	30,827	17.41
Q. Sophia Str.	510	184,502	14.05	504	184,425	14
Dep. of Civil Eng.	70	27,645	14	151	13,385	18.82
Kimmeria	480	128,595	15.3	490	128,468	15.4
Evripidou	50	8,579	17.12	128	-10,268	21+
Orestias	60	17,169	15.27	177	-10,073	21+

2) EFFECT OF PV MODULE COST

The effect of the PV module cost is of primary importance for the techno-economic assessment of the NEM policy viability. Technological advancements and the growing global solar module demand lead to a continuous PV market price reduction [40]. In this context, the average PV module cost in the range of 50 kW to 1000 kWp is assumed equal to 550 €/kW (original case), 525 €/kW (4.5 % reduction) and 500 €/kW (9.1 % reduction). Note that, for the last two cases proper modifications to (17) have been applied.

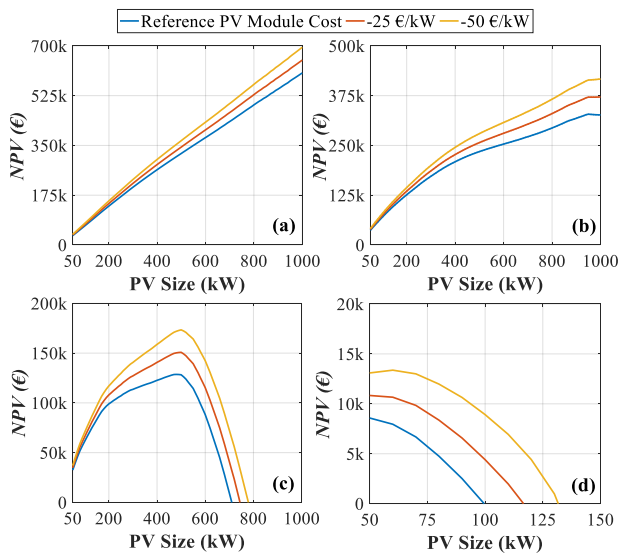

FIGURE 15. ***NPV* as a function of *PV_{size}* for various PV module costs for campus of (a) Komotini, (b) Makri, (c) Kimmeria and (d) Evripidou.**

In Fig. 15, the *NPV* variation against PV_{size} is illustrated indicatively for the campuses of Komotini, Makri, Kimmeria and Evripidou. It is evident that *NPV* increases with decreasing PV module cost. Specifically, by analyzing the calculated *NPV* for all campuses, it can be deduced that a 4.5 % cost reduction results into an increase of the maximum *NPV* in the range of 7.46 % to 26.30 %. Doubling the cost reduction to 9.1 % yields an increase of the maximum *NPV* in the range of 14.92 % to 55.85 %. Generally, the lower *NPV* increase is observed for Komotini, i.e., the campus presenting the highest demand. On the other hand, the most significant increase profit is recorded for Evripidou, i.e., the campus presenting the lowest demand. Considering the results for all nine campuses, it can be deduced that for the majority of the campuses as the PV module cost decreases the optimal PV_{size} (knee of *NPV* curve) increases compared to the original case (see Table VI).

C. EARLY-STAGE SCENARIO

1) QUASI-STATIC SIMULATIONS

The off-grid analysis provides useful information regarding the cost-efficiency of the NEM policy in MV prosumers. However, in order to accurately evaluate the viability of the investment, also the network topology as well as the effect of the PV operational properties should be also considered in the analysis. In this context, the techno-economic assessment is combined with quasi-static simulations.

The quasi-static analysis is performed by using the simulation model of Fig. 4. A network configuration characterized by low PV penetration, namely, early-stage scenario, is examined. In particular, the PV_{size} of the three PV stations is 100 kW. The PV_{size} of the campuses is varied individually from 50 to 1000 kW; for each case the PV_{size} of the remaining eight campuses is equal to the optimal one as derived by the off-grid calculations (Table VI). Note that, network operation is achieved without violating the minimum (0.95 pu) and maximum (1.05 pu) permissible voltage limits [42]. The PV module cost is calculated according to (17). The application of *Q*(*V*) voltage regulation to campus PV systems and PV power stations, as the most commonly used, is examined assuming $\mathbf{QV}_1$={0.95 pu, 0.96 pu, 1.04 pu, 1.05 pu}. Results are compared to those obtained for the business-as-usual case, namely, 'Unity Power Factor' (*UPF*), i.e., no control strategy is incorporated to PV systems.

SCR and *SSR* calculations for both control strategies are similar to those shown in Figs. 8(a), 8(b), 9(a) and 9(b), thus are not presented. This is due to the fact that the prosumer's real power is not influenced by the *Q*(*V*) voltage regulation

This work is licensed under a Creative Commons Attribution-NonCommercial-NoDerivatives 4.0 License. For more information, see https://creativecommons.org/licenses/by-nc-nd/4.0/

This article has been accepted for publication in a future issue of this journal, but has not been fully edited. Content may change prior to final publication. Citation information: DOI 10.1109/ACCESS.2021.3073780, IEEE Access

TABLE VII
NPV ACCORDING TO *Q*(*V*) METHOD FOR DIFFERENT VOLTAGE THRESHOLDS

Campus	PV_{size} (kW)	*NPV* (€)	*Difference (%)*	
		$\mathbf{QV}_1$	$\mathbf{QV}_2$={0.95 pu, 0.97 pu, 1.03 pu, 1.05 pu}	$\mathbf{QV}_3$={0.95 pu, 0.98 pu, 1.02 pu, 1.05 pu}
Komotini	1000	604,486	-1.06	-3.71
Tsaldari	110	21,805	+0.38	-0.05
Makri	950	325,832	-0.54	-1.71
Chili	100	42,887	+0.56	+1.09
Q. Sophia Str.	510	184,465	-0.76	-4.46
Dep. of Civil Eng.	70	27,646	-0.06	-0.79
Kimmeria	480	128,428	-0.41	-1.70
Evripidou	50	8,572	-0.22	-1.05
Orestias	60	9,942	-46.83	-65.08

scheme. Moreover, *UPF* results practically coincide with those obtained by the off-grid analysis. The difference in *NPV* and *IRR* between the control strategies is depicted in Figs. 16 and 17, respectively. In these figures, results are presented for cases of PV_{size} yielding positive *NPV* under the *UPF* method. It can be deduced that significant differences are observed mainly for the Orestias campus, since *NPV* for *UPF* is significantly higher than that of *Q*(*V*) (reaching ~16k €). In particular, the mean power factor for the *UPF* and *Q*(*V*) methods is 0.91 and 0.65, respectively. In this sense, the electricity charges under the *Q*(*V*) control are higher yielding decreased investment profitability and *IRR*. Regarding *DPP* and *ROI*, corresponding differences have been observed for the two control strategies; results present the same behaviour as those shown in Figs. 12 and 13, respectively, thus will not be presented. Finally, note that, *LCOE* depends on the total energy yield of the PV system during the lifetime of the investment as well as on the PV geographical location. This implies that *LCOE* remains constant, regardless the operational conditions.

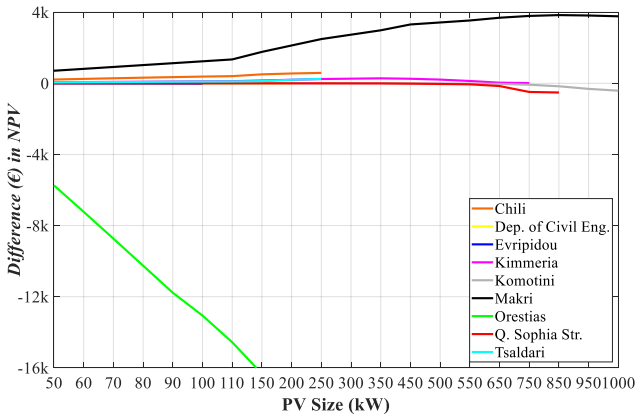

FIGURE 16. ***NPV* difference as a function of PV_{size}.**

2) EFFECT OF *Q*(*V*) OPERATIONAL PROPERTIES

The annual voltage at node No. 22 of Orestias campus presents a variation between 1.04 and 1.05 pu for the 95 % of the year. This necessitates a significant absorption of reactive power for voltage regulation in terms of the *Q*(*V*) operational properties, influencing the net reactive power of the prosumer; hence, its energy billing.

In this context, in Table VII the impact of the *Q*(*V*) voltage regulation properties on the prosumer's *NPV* is analyzed for cases $\mathbf{QV}_1$, $\mathbf{QV}_2$ and $\mathbf{QV}_3$ and the % differences with reference to $\mathbf{QV}_1$ are calculated. Details on $\mathbf{QV}_2$ and $\mathbf{QV}_3$ are given in Table VII. Simulations are performed assuming the optimal PV_{size} (Table VI). In general, as the *Q*(*V*) voltage deactivation range V_2 to V_3 decreases, the *NPV* for the majority of the campuses decreases. In this sense, significant impact on *NPV* is mainly observed for Orestias campus; differences can be also indicated for Komotini and Q. Sophia Str. for $\mathbf{QV}_3$. It should be noted that, contrary to most of the examined cases, a beneficial economic impact of the application of *Q*(*V*) is observed for the Chili campus as the voltage range decreases. This is attributed to the fact that *Q*(*V*) regulation improves the prosumer's power factor.

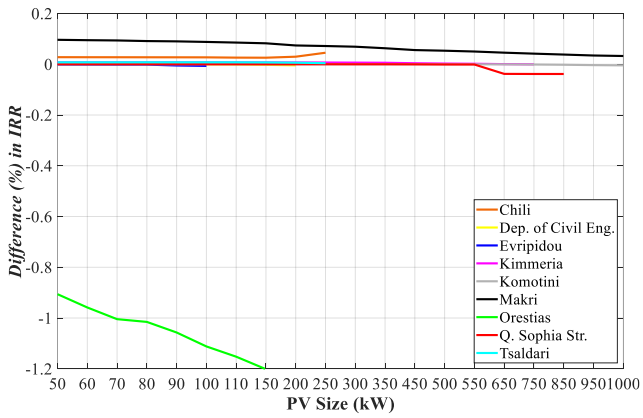

FIGURE 17. ***IRR* difference as a function of PV_{size}.**

D. HIGH PENETRATION SCENARIO

Next, the high PV penetration scenario is examined. The PV_{size} of the three PV power stations is 700 kWp and voltage violations occur; thus, the application of voltage regulation strategies to PV systems is important. Quasi-static analysis is performed by examining the

This work is licensed under a Creative Commons Attribution-NonCommercial-NoDerivatives 4.0 License. For more information, see https://creativecommons.org/licenses/by-nc-nd/4.0/

This article has been accepted for publication in a future issue of this journal, but has not been fully edited. Content may change prior to final publication. Citation information: DOI 10.1109/ACCESS.2021.3073780, IEEE Access

cosφ(P), Q(P) and Q(V) controls. To demonstrate in detail the effect of the voltage regulation methods on *NPV*, comparisons are carried out by employing the difference in *NPV* as follows:

$$diff\,(€) = NPV_{cos\varphi(P)/Q(P)} - NPV_{Q(V)} \tag{18}$$

Results are summarized in Fig. 18, revealing that the same optimal PV_{size} is obtained for all control strategies. Note that, by applying the voltage control strategies network voltages are maintained within the permissible limits. However, generally differences in *NPV* can be observed; the highest *NPV* for most of the cases is obtained by applying the Q(V) control strategy. This is not the case for Orestias, Evripidou and Tsaldari campuses, since the application of the cosφ(P) control results into higher power factor, thus being the most profitable. Based on the above, it can be concluded that both the network and the prosumer's operational properties influence significantly the campus power factor and consequently the viability of the NEM policy.

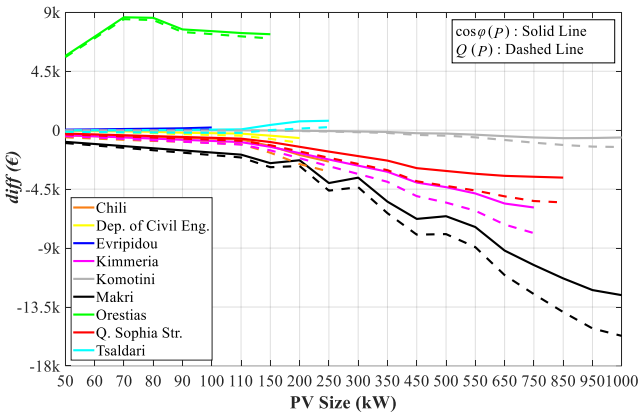

FIGURE 18. ***diff*(€) as a function of *PV*$_{size}$.**

The cost-efficiency of the NEM policy between the 'high penetration' and the 'early-stage' scenarios is compared in Fig. 19. In particular, the difference between the maximum *NPV* calculated for the cosφ(P), Q(P) and Q(V) controls for the 'high penetration' scenario and the maximum *NPV* for the *UPF* (reference) for the 'early stage' are presented in Fig. 19(a). The corresponding difference assuming Q(V) control (for set **QV**$_1$) of the 'early stage' as reference are presented in Fig. 19(b). It is evident, that the increased PV penetration yields lower profits to prosumers incorporating voltage regulation controls. This is attributed to their activation to mitigate relevant network voltage violations. Note that, the positive % differences observed in Fig. 19(b) are associated to the lower *NPV* of Orestias campus, when Q(V) method is employed.

VIII. CONCLUSIONS

The present work introduces a generalized methodology that provides the means for assessing the viability of the

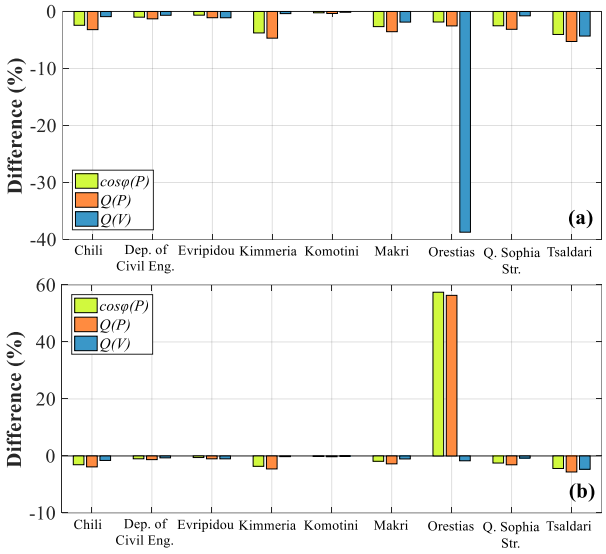

FIGURE 19. **Differences (%) of maximum *NPVs* with reference to (a) *UPF* and (b) *Q*(*V*) method.**

NEM policy in MV prosumers. This was achieved by combining techno-economic analysis with quasi-static simulations, improving the accuracy of the evaluation. By using the proposed methodology, an investigation of the effect of the PV size, PV cost, voltage regulation control strategy and relevant operational properties on the viability of the NEM policy has been conducted. The developed code in MATLAB of the proposed methodology and the data used in Section VII are available in [43].

The application of the proposed methodology to university campus prosumers under the NEM policy in Greece has shown that:

1) NEM policy may constitute a very profitable investment, especially for MV prosumers presenting high demand. This is not the case for MV prosumers presenting generally low demand. In these cases, the revenue of the prosumer during the lifetime period is not significant compared to the investment capital cost.
2) The decreasing trend in PV system costs eventually improves the cost-efficiency of the NEM investment and also influences the optimal PV sizing; especially for prosumers presenting low demand.
3) Optimal PV sizing for prosumers presenting high demand can be generally determined by applying a simplified approach in terms of equalizing prosumer's produced and consumed energy. However, for prosumers presenting low demand, a more generic method must be followed in terms of *NPV* maximization. The above off-grid analysis approaches provide a good estimate of the optimal PV size, especially when no control strategy is incorporated to PV systems. This is not the case, when voltage regulation control methods are applied to the

This work is licensed under a Creative Commons Attribution-NonCommercial-NoDerivatives 4.0 License. For more information, see https://creativecommons.org/licenses/by-nc-nd/4.0/

This article has been accepted for publication in a future issue of this journal, but has not been fully edited. Content may change prior to final publication. Citation information: DOI 10.1109/ACCESS.2021.3073780, IEEE Access

prosumer's PV system. In such cases, the accurate techno-economic viability assessment necessitates the calculation of the net energy export / import by means of quasi-static simulations, incorporating the real-world operational properties of the distribution network.

4) The operational properties of voltage regulation methods can influence the economic viability of NEM policy. It was found that as the voltage activation range widens, the *NPV* for the majority of the campuses decreases.
5) The increasing DG penetration in distribution networks may reduce prosumer's net income, due to the activation of the voltage regulation controls to mitigate possible voltage violations.
6) The comparative analysis of the $Q(P)$, $\cos\varphi(P)$ and $Q(V)$ voltage regulation techniques generally revealed that, the application of the $Q(V)$ method results into the most beneficial economic impact.
7) Future support mechanisms should offer incentives to the prosumers for the provision of ancillary services, e.g., reactive power support to the grid, to facilitate and further promote the installation of RES.

APPENDIX

A. SUPPLY CHARGES

C_E is calculated according to

$$C_E = C_{EF_A} \cdot E_A + C_{EF_B} \cdot E_B . \quad \text{(A1)}$$

Furthermore, C_P is calculated using either (A2) or (A3). $P_{\max}$ is the peak demand during the day, C_{PF} is the power charge factor, and $P'_{\max}$ is the peak demand during the working day hours (7:00-23:00). Finally, *BPD* is the number of the billing period days.

$$C_P = \frac{1.18 \cdot P_{\max} \cdot C_{PF} \cdot BPD}{30} \quad \text{(A2)}$$

$$C_P = \frac{P'_{\max} \cdot C_{PF} \cdot BPD}{30}. \quad \text{(A3)}$$

The selection between (A2) and (A3) is made by the value of the customer utilization factor (*UF*) which is calculated as follows

$$UF = \frac{E}{24 \cdot BPD \cdot P_{\max}} \quad \text{(A4)}$$

where *E* denotes the total consumed energy within the billing period (E_A+E_B). In case *UF* is less than 0.30, C_P is calculated by means of (A2), while for the rest of the cases according to (A3).

B. REGULATED CHARGES

C_{TN} covers the expenses regarding the operation, maintenance, and development of the transmission system as

$$C_{TN} = \frac{UC \cdot P'_{\max} \cdot BPD}{30}. \quad \text{(A5)}$$

C_{DN} covers the expenses regarding the operation, maintenance, and development of the distribution system and is calculated as

$$C_{DN} = \frac{UC_{fc} \cdot P''_{\max} \cdot BPD}{30} + \frac{E \cdot UC_{vc}}{\cos\varphi} \quad \text{(A6)}$$

where $P''_{\max}$ is the maximum peak demand during 11:00-14:00 of all days of the billing period, *UC* is the energy charge, UC_{fc} is the standard fee, UC_{vc} the variable charge and $\cos\varphi$ the averaged measured power factor. The C_{GhT}, C_{SGI} and C_{OC} are calculated by (A7), (A8) and (A9), respectively.

$$C_{GhT} = UC_{GhT} \cdot E \quad \text{(A7)}$$

$$C_{SGI} = UC_{SGI} \cdot E \quad \text{(A8)}$$

$$C_{OC} = UC_{OC} \cdot E \quad \text{(A9)}$$

where UC_{GhT}, UC_{SGI}, and UC_{OC} are the C_{GhT}, C_{SGI} and C_{OC} charges (€) per kWh, respectively.

C. MUNICIPAL FEES AND TAXES

The municipal fees (C_{MF}) and municipal taxes (C_{MT}) are calculated by means of (A10) and (A11), respectively. $C_{municipal}$ is obtained by adding also to the above charges the VAT.

$$C_{MF} = \frac{S \cdot K_{MF} \cdot BPD}{365} \quad \text{(A10)}$$

$$C_{MT} = \frac{S \cdot K_{MT} \cdot BPD}{365} \quad \text{(A11)}$$

where *S* is the surface of the installation and K_{MF}, K_{MT} are auxiliary fixed factors.

REFERENCES

[1] European Commision, "Directive (EU) 2009/28/EC of the European Parliament and of the Council of 23 April 2009 on the promotion of the use of energy from renewable sources and amending and subsequently repealing directives 2001/77/EC and 2003/20/EC," Apr. 2009
[2] European Commision, "Directive (EU) 2018/2001 of the European Parliament and of the Council of 11 December 2018 on the promotion of the use of energy from renewable sources," Dec. 2018.
[3] Eurostat, "Renwable Energy statictics – Statictics Explained", Available: https://ec.europa.eu/eurostat/statistics-explained/index.php/Renewable_energy_statistics
[4] R. de Oliveira Azevêdo, P. Rotela Junior, L. C. S. Rocha, G. Chicco, G. Aquila, and R. S. Peruchi, "Identification and Analysis of Impact Factors on the Economic Feasibility of Photovoltaic

This work is licensed under a Creative Commons Attribution-NonCommercial-NoDerivatives 4.0 License. For more information, see https://creativecommons.org/licenses/by-nc-nd/4.0/

This article has been accepted for publication in a future issue of this journal, but has not been fully edited. Content may change prior to final publication. Citation information: DOI 10.1109/ACCESS.2021.3073780, IEEE Access

Energy Investments," *Sustainability*, vol. 12, no. 17, pp. 7173, Sep. 2020.

[5] A. I. Nikolaidis and C. A. Charalambous, "Hidden financial implications of the net energy metering practice in an isolated power system: Critical review and policy insights," *Renewable and Sustainable Energy Reviews*, vol. 77, pp. 706-717, Sep. 2017.

[6] I. D'Adamo, M.Gastaldi and P. Morone, "The post COVID-19 green recovery in practice: Assessing the profitability of a policy proposal on residential photovoltaic plants," *Energy Policy*, vol. 147, 111910, Dec. 2020.

[7] G. C. Christoforidis, I. P. Panapakidis, T. A. Papadopoulos, G. K. Papagiannis, I. Koumparou, M. Hadjipanayi, and G. E. Georghiou, "A model for the assessment of different net-metering policies," *Energies*, vol. 9, no. 4, 262, Jan. 2016.

[8] I. Koumparou, G. C. Christoforidis, V. Efthymiou G. K. Papagiannis, and G. E. Georghiou, "Configuring residential PV net-metering policies - A focus on the Mediterranean region," *Renew. Energy*, vol. 113, pp. 795-812, Dec. 2017.

[9] R. Dufo-López and J. L. Bernal-Agustín, "A comparative assessment of net metering and net billing policies. Study cases for Spain," *Energy*, vol. 84, pp 684-694, May 2015.

[10] R. Górnowicz and R. Castro, "Optimal design and economic analysis of a PV system operating under Net Metering or Feed-In-Tariff support mechanisms: A case study in Poland," Sustainable Energy Technologies and Assessments, vol. 42, 100863, Dec. 2020.

[11] Law 4203/2013 (Government Gazette A 235 / 1-11-2013), Regulations on Renewable Energy Sources and other provisions.

[12] IRENA, "Innovation landscape brief: Net billing schemes, International Renewable Energy Agency," 2019.

[13] Hellenic Association of Photovoltaic Companies, "Net-metering," 2019.

[14] A. Colasante, I. D'Adamo and P. Morone, "Nudging for the increased adoption of solar energy? Evidence from a survey in Italy," *Energy Research & Social Science*, vol. 74, 101978, Apr. 2021.

[15] S. Sukumar, H. Mokhlis, S. Mekhilef, M. Karimi, and S. Raza, "Ramp-rate control approach based on dynamic smoothing parameter to mitigate solar PV output fluctuations," *Int. J. Elect. Power Energy Syst.*, vol. 96, pp. 296–305, Mar. 2018.

[16] G. C. Kryonidis, E. O. Kontis, A. I. Chrysochos, C. S. Demoulias, and G. K. Papagiannis, "A coordinated droop control strategy for overvoltage mitigation in active distribution networks," *IEEE Trans. Smart Grid*, vol. 9, no. 5, pp. 5260–5270, Sep. 2018.

[17] A. I. Nousdilis, G. C. Christoforidis, and G. K. Papagiannis, "Active power management in low voltage networks with high photovoltaics penetration based on prosumers' self-consumption," *Applied Energy*, vol. 229, pp. 614–624, Nov. 2018.

[18] S. Robak, J. MacHowski, and K. Gryszpanowicz, "Automatic alleviation of overloads in transmission network by generation curtailment," *IEEE Trans. Power Syst.*, vol. 33, no. 4, pp. 4424–4432, Jul. 2018.

[19] C. L. Masters, "Voltage rise: the big issue when connecting embedded generation to long 11 kV overhead lines," *Power Eng. J.*, vol. 16, no. 1, pp. 5–12, Feb. 2002.

[20] T. Stetz, F. Marten, and M. Braun, "Improved low voltage grid integration of photovoltaic systems in Germany," *IEEE Trans. Sustain. Energy*, vol. 4, no. 2, pp. 534–542, Apr. 2013.

[21] G. C. Kryonidis, C. S. Demoulias, and G. K. Papagiannis, "A nearly decentralized voltage regulation algorithm for loss minimization in radial MV networks with high DG penetration," *IEEE Trans. Sustain. Energy*, vol. 7, no. 4, pp. 1430–1439, Oct. 2016.

[22] R. Tonkoski, L. A. C. Lopes, and T. H. M. El-Fouly, "Coordinated active power curtailment of grid connected PV inverters for overvoltage prevention," *IEEE Trans. Sustain. Energy*, vol. 2, no. 2, pp. 139-147, Apr. 2011.

[23] A. Samadi, R. Eriksson, L. Soder, B. Rawn, and J. Boemer, "Coordinated active power-dependent voltage regulation in distribution grids with PV systems," *IEEE Trans. Power Del.*, vol. 29, no. 3, pp.1454–1464, Jun. 2014.

[24] S. Conti, A. Greco, N. Messina, and S. Raiti, "Local voltage regulation in LV distribution networks with PV distributed generation," presented at *Int. Symp. Power Electron., Elect. Drives, Autom. and Motion*, May 2006, pp. 519–524.

[25] G. Kryonidis, C. Demoulias, and G. Papagiannis, "A probabilistic evaluation of voltage control strategies in active MV networks," presented at *52nd Int. Univ. Power Eng. Conf. (UPEC)*, 2017, pp. 1-6.

[26] A. Samadi, E. Shayesteh, R. Eriksson, B. Rawn, and L. Soder, "Multiobjective coordinated droop-based voltage regulation in distribution grids with PV systems," *Renew. Energy*, vol. 71, pp. 315–323, Nov. 2014.

[27] A. Nousdilis, G. Kryonidis, E. Kontis, G. K. Papagiannis, G. C. Christoforidis, and I. P. Panapakidis, "Economic viability of residential PV systems with battery energy storage under different incentive schemes," presented at *IEEE Int. Conf. Environment and Elect. Eng.* And *IEEE Ind. Com. Power Syst. Europe (EEEIC / I&CPS Europe)*, Palermo, 2018.

[28] M. Preuss, "Return on investment and grants: A Review of present understandings and recommendations for change," *Research Management Review*, vol. 21, no. 1 2016.

[29] R. Opoku, G. Obeng, E. Adjei, F. Davis, and F. Akuffo, "Integrated system efficiency in reducing redundancy and promoting residential renewable energy in countries without net-metering: A case study of a SHS in Ghana," *Renew. Energy*, vol. 155, pp 65-78, Aug. 2020.

[30] D. Shaw-Williams and C. Susilawati, "A techno-economic evaluation of Virtual Net Metering for the Australian community housing sector," *Applied Energy*, vol. 261, Mar. 2020.

[31] A. Nousdilis, G. Kryonidis, E. Kontis, G. Barzegkar-Ntovom, I. P. Panapakidis, G. C. Christoforidis, and G. K. Papagiannis, "Impact of policy incentives on the promotion of integrated pv and battery storage systems: A Techno-economic assessment," *IET Renew. Power Gener.*, vol. 14, no. 7, pp. 1174-1183, May 2020.

[32] K. Pippi, T. Papadopoulos, and G. Kryonidis, "Viability assessment of PV systems in university campuses under the net-metering policy," presented at *55nd Int. Univ. Power Eng. Conf. (UPEC)*, 2020, pp. 1-6.

[33] Public Power Corporation SA-Hellas, Available: https://www.dei.gr/el

[34] R. Kabiri, G. Holmes, and B. Mcgrath, "The influence of pv inverter reactive power injection on grid voltage regulation," at *5th IEEE Int. Symp. Power Electron. Distributed Generation Syst.*, pp.1-8, 2014.

[35] R. Luthander, J. Widén, D. Nilsson, and J. Palm, "Photovoltaic self-consumption in buildings: A review," *Applied Energy*, vol. 142, pp. 80-94, Mar. 2014.

[36] R. C. Dugan and D. Montenegro, "Reference Guide – The Open Distribution System Simulator," Electric Power Research Institute Inc., 2020.

[37] M. E. Baran and F. F. Wu, "Network reconfiguration in distribution systems for loss reduction and load balancing," *IEEE Trans. Power Del.*, vol. 4, pp. 1401–7, Apr. 1989.

[38] A. I. Nousdilis, A. I. Chrysochos, G. K. Papagiannis, and G. C. Christoforidis, "The impact of photovoltaic self-consumption rate on voltage levels in LV distribution grids," presented at *IEEE Int. Conf. Compatibility, Power Electronics and Power Engineering*, 2017, pp. 650–655.

[39] T. A. Papadopoulos, G. T. Giannakopoulos, V. C. Nikolaidis, A. S. Safigianni, and I. P. Panapakidis, "Study of electricity load profiles in university campuses: The case study of Democritus University of Thrace," presented at *Med. Conf. Power Gener., Trans., Distrib. Energy Conv. (MedPower 2016)*, Belgrade, 2016.

[40] S. Pfenninger, I. Staffell, Renewables.ninja, Available: https://www.renewables.ninja/

[41] A. Jäger-Waldau, "PV Status Report 2019," JRC Science for policy report, https://ec.europa.eu/jrc/sites/jrcsh/files/kjna29938enn_1.pdf

[42] G. C. Kryonidis, N. V. Theologou, A. I. Chrysochos, C. S. Demoulias, and G. K. Papagiannis, "An enhanced decentralized voltage regulation scheme for the reduction of tap changes in HV/MV transformers under high DG penetration", presented at *IEEE PES Innov. Smart Grid Tech. Conf. Europe (ISGT-Europe)*, 2016, p.p 1-6.

[43] [Online]. Available: https://activate.ee.duth.gr/downloads

This work is licensed under a Creative Commons Attribution-NonCommercial-NoDerivatives 4.0 License. For more information, see https://creativecommons.org/licenses/by-nc-nd/4.0/

This article has been accepted for publication in a future issue of this journal, but has not been fully edited. Content may change prior to final publication. Citation information: DOI 10.1109/ACCESS.2021.3073780, IEEE Access

KALLIOPI D. PIPPI (S'20) was born in Xanthi on 4th of July 1996. In 2014 she started her studies at the Department of Electrical and Computer Engineering of Democritus University of Thrace, Xanthi, Greece, from where she graduated in July 2019.

Since December 2019, she has been a PhD candidate at the Department of Electrical and Computer Engineering of Democritus University of Thrace. Her main research interests during her post-graduate studies are related to the ancillary service solutions for Transmission and Distribution System Operators.

Ms Pippi was a recipient of the MedPower2020 Best Paper Award at MedPower 2020 Conference.

GEORGIOS C. KRYONIDIS (S'12–M'18) received the Dipl. Eng. and Ph. D. degrees from the School of Electrical and Computer Engineering at the Aristotle University of Thessaloniki, Greece, in 2013 and 2018, respectively. Currently, he is an adjunct Lecturer at the same University. He has an 8-year experience as a researcher in EU research projects (FP7, H2020, Interreg-Med). His research interests include, distributed generation and storage, renewable energy sources, microgrids, and smart grids operation and control.

THEOFILOS A. PAPADOPOULOS (S'01–M'09–SM'18) received the Dipl. Eng. and Ph.D. degrees from the School of Electrical and Computer Engineering, Aristotle University of Thessaloniki, Thessaloniki, Greece, in 2003 and 2008, respectively. He is currently an Assistant Professor with the Power Systems Laboratory, Department of Electrical and Computer Engineering, Democritus University of Thrace, Komotini, Greece. His research interests include power systems modeling, power line communication, and computation of electromagnetic transients.

Dr. Papadopoulos received the Basil Papadias Award at the IEEE PowerTech '07 Conference.

This work is licensed under a Creative Commons Attribution-NonCommercial-NoDerivatives 4.0 License. For more information, see https://creativecommons.org/licenses/by-nc-nd/4.0/